differing only by the station constant (the bracketted term) from the rough expression (13). We have to bear in mind that sign (l_r) = sign (Δt_{S0}) in using Eq. (21) to determine l_r. Formulae (21) and (12) should be employed together with the formulae of the Fresnel characteristics theory in establishing the radiant position. But to work this theory requires the cosine of the zenith distance of the radiant, $\cos z_R$, to be known. Therefore, we first have to determine $\cos z_R$ from the classical theory embodied by Kashcheev et al. (1967) formula. We can then evaluate $\cos z_R$ using our formulae with the deceleration parameters of the meteoroid determined from Pecina's theory (1988). This new value of $\cos z_R$ can generate a more precise value of l_r based on this deceleration theory. The iteration procedure is to be repeated until the prescribed accuracy of parameters in question is reached.

We can conclude that we have derived the formulae enabling the position of the radiant of decelerating meteoroid to be determined.

REFERENCES

Andrianov N. S., Sidorov V. V. 1983 *Meteornoe rasprostranenie radiovoln* **18**, 25

Born M., Wolf E. 1973 *Principles of Optics* (russian translation, Nauka, Moskva), p. 132

Kashcheev B. L., Lebedinets V. N., Lagutin M. F. 1967 Rezul'taty Issled. IGY, Issled. Meteorov No. 2, p. 149

Pecina P. 1988 *Bull. Astron. Inst. Czechosl.* **39**, 193

Pecina P., Ceplecha Z. 1984 *Bull. Astron. Inst. Czechosl.* **35**, 120

ATMOSPHERIC EXCITATION OF EARTH'S ROTATION: COMPARISON OF THE SPECTRUM OF THE LENGTH-OF-DAY AND AXIAL COMPONENT OF THE ANGULAR MOMENTUM FUNCTION OF THE ATMOSPHERE

N. Pejović[1]), J. Vondrák[2])

1) *Astronomical Institute, Mathematical Faculty, University of Belgrade, Studentski trg 16, 11000 Beograd, Yugoslavia*

2) *Astronomical Institute, Czechoslovak Academy of Sciences, Budečská 6, 120 23 Praha 2, Czechoslovakia*

Received 8 December 1988

АТМОСФЕРНОЕ ВОЗБУЖДЕНИЕ ВРАЩЕНИЯ ЗЕМЛИ: СРАВНЕНИЕ СПЕКТРОВ ДЛИНЫ СУТОК И ОСЕВОЙ СОСТАВЛЯЮЩЕЙ ФУНКЦИИ МОМЕНТА КОЛИЧЕСТВА ДВИЖЕНИЯ АТМОСФЕРЫ

В статье показано, что наблюдаемые изменения длины суток можно для периодов от 10 до 180 суток полностью объяснить комбинированным воздействием перераспределения момента количества движения между Землей и ее атмосферой, и приливных деформаций фигуры Земли. Найдено значение шкального фактора приливных влияний $k/C = 0{,}945 \pm 0{,}021$. Малые несоответствия между наблюдаемыми и возбужденными амплитудами основных полугодовых и годовых членов могут быть, с большой вероятностью, вызваны влиянием зональных ветров в стратосфере, которыми обычно пренебрегают при вычислении моментов количества движения атмосферы. С другой стороны, долгопериодические составляющие в длине суток (с периодами 2,4 года и 6,0 года) не могут быть объяснены ни одим из обоих рассматриваемых влияний.

It is shown that the fluctuations observed in length-of-day, for periods from 10 to 180 days, can be fully explained by the combined effect of the redistribution of angular momentum between the Earth and its atmosphere, and tidal deformations of the Earth's body. The tidal effect scaling factor k/C is found to be equal to $0{\cdot}945 \pm 0{\cdot}021$. The small discrepancies between the observed and excited amplitudes of the dominating semi-annual and annual terms can very probably be caused by the influence of zonal stratospheric winds, neglected in the routinely calculated atmospheric angular momentum functions. On the other hand, the observed long-periodic components in the length-of-day (with periods of 2·4 y and 6·0 y) cannot be explained by any of the two discussed influences.

Key words: Rotation of the Earth — atmospheric excitation — Earth tides

1. Introduction

It has become a well-known fact that the exchange of angular momentum between the atmosphere and solid Earth plays a dominant role in the changes of Earth rotation parameters (polar motion, length-of-day). The earlier results and theoretical considerations of the problem can be found e.g. in two principal monographs, devoted to the rotation of the Earth, by Munk and MacDonald (1960) and by Lambeck (1980). Many papers have since been devoted to the problem. The seasonal variations (annual, semi-annual) in the length-of-day (LOD) were proved to be caused mainly by the combined effect of the atmosphere and tides – see, e.g., Lambeck and Cazenave (1973, 1974, 1977), Sidorenkov (1973 and 1979) Rosen and Salstein (1983) or Eubanks et al. (1985). Feissel and Nitschelm (1985) proved that the recently found short-peripdic fluctuations (with periods between 50 and 70 days) in LOD are closely correlated to the variations in the axial component of the relative angular momentum of the atmosphere within the same frequency band. Djurović and Pâquet (1988) showed that the origin of these fluctuations lies very probably in physical processes in the Sun. A recent overview of the problem and discussion of the prospects was presented by Dickey and Eubanks (1987). The "effective angular momentum functions" (EAMF) of the atmosphere, proposed by Barnes et al. (1983), have been accepted worldwide and are now routinely calculated by several meteorological centers daily, and after 1984 even twice daily. On the other hand, the measured Earth rotation parameters are known, thanks to modern techniques of observation, with ever increasing precision. This enables these data to be used for detailed analysis in order to estimate to what extent the LOD changes are caused by the atmosphere and which part is left to other influences. In the following, we shall first compare the spectra of the observed LOD changes and atmospheric EAMF, and then try to find a simple functional relation between the observed LOD, on the one hand, and atmospheric EAMF and zonal luni-solar tides, on the other.

2. The Input Data Sets and their Spectral Analysis

The following data sets have been used for the subsequent spectral analysis, in the interval 1976·5 to 1986·0:

a) The observed rate of the Earth's rotation was represented by the series of raw 5-day values of UT1-TAI (i.e. the difference between the rotational and atomic time scale) as derived by the Bureau International de l'Heure in Paris from the combination of all available observations, both from optical astrometry and modern space techniques (BIH 1976–1985, Tab. 6). The numerical differentiation of this time series has further been used to derive the corresponding values of the length-of-day excess over its nominal value (86 400 sec) in seconds of time:

$$\text{LOD} = -\partial(\text{UT1} - \text{TAI})/\partial t\,, \tag{1}$$

where the time derivative on the rhs is reckoned in seconds per day. Since we are mainly interested in periods of less than several years, namely this last data set was used instead of the original UT1 – TAI values (differentiation of a time series amplifies the amplitudes of its short-periodic part while suppressing its long-term changes).

b) The axial component of the effective angular momentum function (EAMF) of the atmosphere, introduced by Barnes et al. (1983), is a dimensionless quantity; its so-called pressure term is

$$\chi_3^p = \frac{0{\cdot}70R^4}{gC_m}\int_S p_s \cos^3\varphi\,\mathrm{d}\varphi\,\mathrm{d}\lambda. \tag{2}$$

It expresses the influence of the redistribution of air mass on the principal moment of inertia of the whole Earth. The axial component of the wind term

$$\chi_3^W = \frac{1{\cdot}00R^3}{g\Omega C_m}\int_V u\cos^2\varphi\,\mathrm{d}\varphi\,\mathrm{d}\lambda\,\mathrm{d}p \tag{3}$$

expresses the relative angular momentum of the atmosphere (with respect to the rotating solid body of the Earth). The subscript S denotes integration over the whole surface of the Earth and V over the volume of the atmosphere, φ, λ and p geographical latitude, longitude and air pressure, respectively. The symbol p_s denotes atmospheric surface pressure (not reduced to mean sea level), u is the eastward component of the wind velocity. $R = 6370$ km is the mean Earth's radius, $C_m = 7{\cdot}04 \times 10^{37}$ kg m^2 is the axial moment of inertia of the Earth's mantle (the core being considered decoupled from the mantle), $g = 9{\cdot}81$ m s^{-2} is the average gravitational acceleration at the Earth's surface and $\Omega = 6{\cdot}3004$ rad/day denotes the mean rotational velocity of the Earth. The pressure term is also calculated with the so-called "inverted barometer" (IB) correction; the reaction of the ocean to the air pressure changes is supposed to compensate these changes in such a manner that the total atmospheric and ocean effect is constant over the whole surface of each ocean. The EAMF as calculated by the U.S. National Meteorological

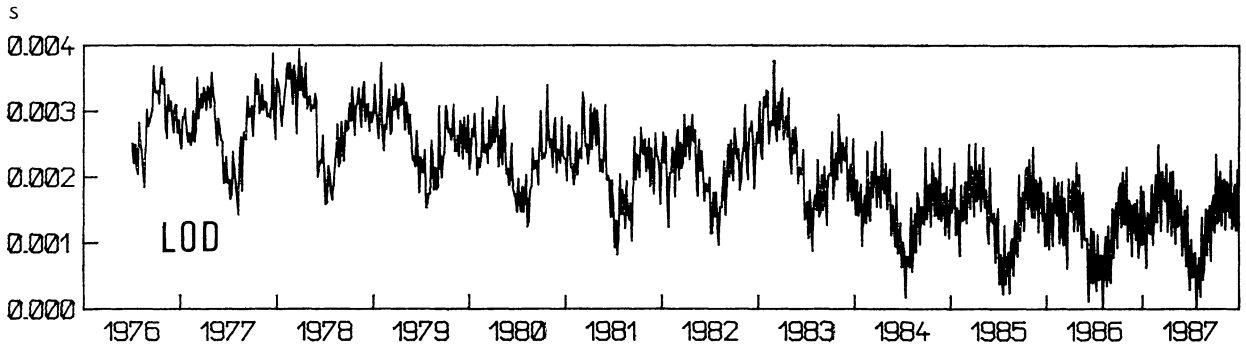

Fig. 1. The excess of length-of-day over the nominal 86 400 sec, calculated from the BIH combined solution. The raw data UT 1 — TAI have been used.

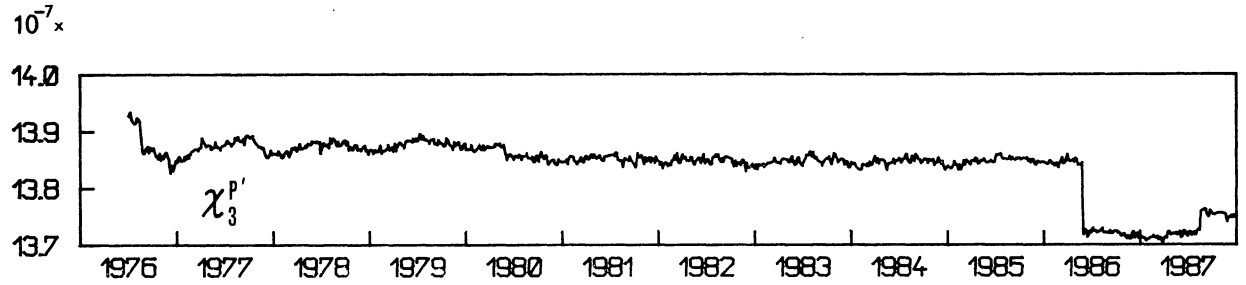

Fig. 2. The axial component of the pressure term of the atmospheric EAMF with the IB correction as determined by the NMC.

Center (NMC) and provided by courtesy of F. W. Fallon (1986) of the National Geodetic Survey and D. Gambis (1988) of the Central Bureau of the IERS has been used.

The data sets are graphically displayed, in the time domain, in Figs 1—4. Figure 1 shows the excess of the LOD over the nominal 86 400 sec; its complex periodic character is mainly due to the combined effects of the atmosphere with the variations caused by the zonal tides of the Earth (Yoder et al. 1981). In order not to suppress the short-periodic tidal variations (with dominating fortnightly and monthly terms), in differentiating the original UT1 — TAI data, the theoretical tides in UT1 with periods shorter than 35 days (i.e. the first 41 terms of Yoder's list) were first removed from UT1 — TAI. These values were then differentiated with respect to time, and only then were the tides in LOD added to obtain the final LOD data set. The scaling factor $k/C = 0{\cdot}94$, recommended by Yoder et al. (1981), has been used to account for the elasticity of the mantle and the effect of the ocean. Since there is no substantial difference (save for a small constant shift) between χ_3^P and $\chi_3^{P'}$ (pressure term without and with the IB correction, respectively), only $\chi_3^{P'}$ is illustrated in Fig. 2. Notice the sudden jump of about $0{\cdot}136 \times 10^{-7}$ in the May 1986 data, due to the change in the forecast model used by the NMC (Salstein 1987). It can be seen that this term does not contribute very much to the total effect, if compared with the wind term in Fig. 3 and the combination of both $(\chi_3^W + \chi_3^{P'})$ in Fig. 4, where the discontinuity mentioned above is less obvious.

The spectral analysis of these data sets (from which the jump in the pressure term has been removed) was carried out using two different methods, in order to estimate which periods are real, and to what extent and at which frequencies the LOD is influenced by the atmosphere. Since the data were sampled at 5-day intervals, only periods longer than 25 days

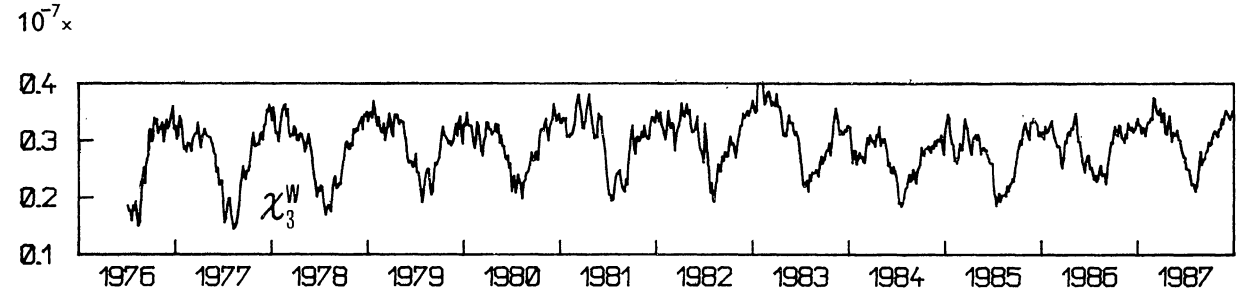

Fig. 3. The axial component of the wind term of the atmospheric EAMF as determined by the NMC.

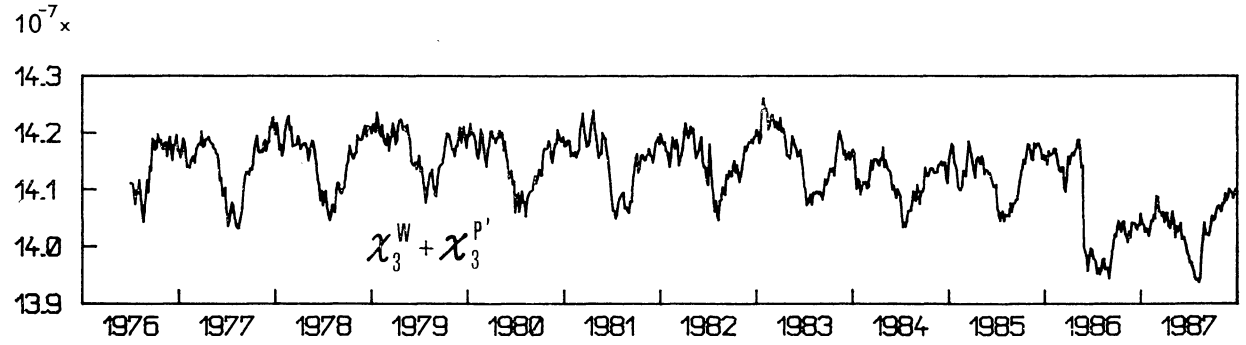

Fig. 4. The axial component of the sum of the pressure and wind terms of the atmospheric EAMF as determined by the NMC.

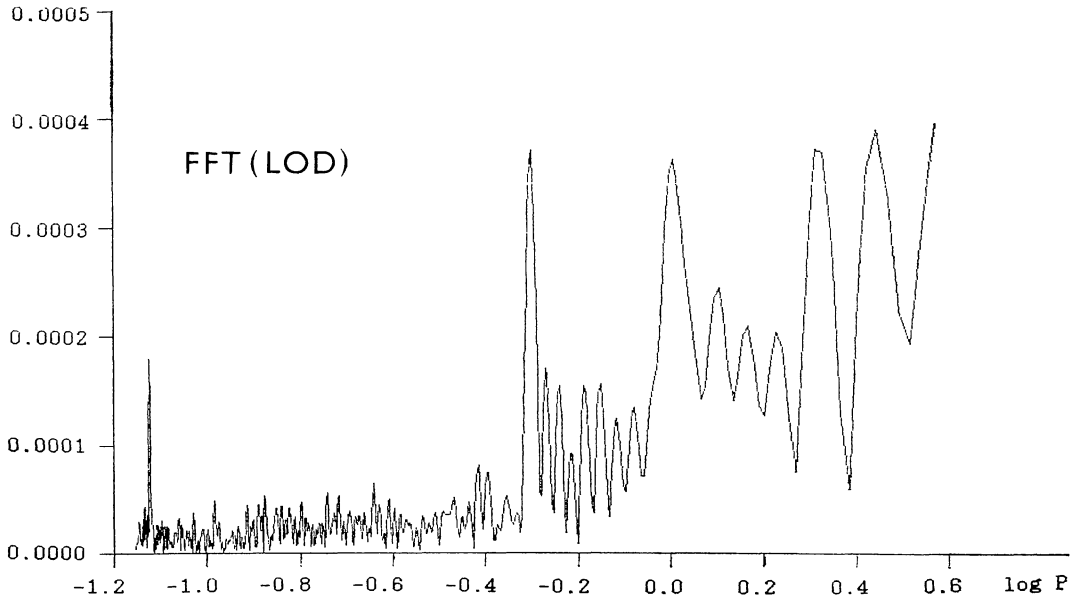

Fig. 5. The spectrum of the observed LOD calculated by the FFT.

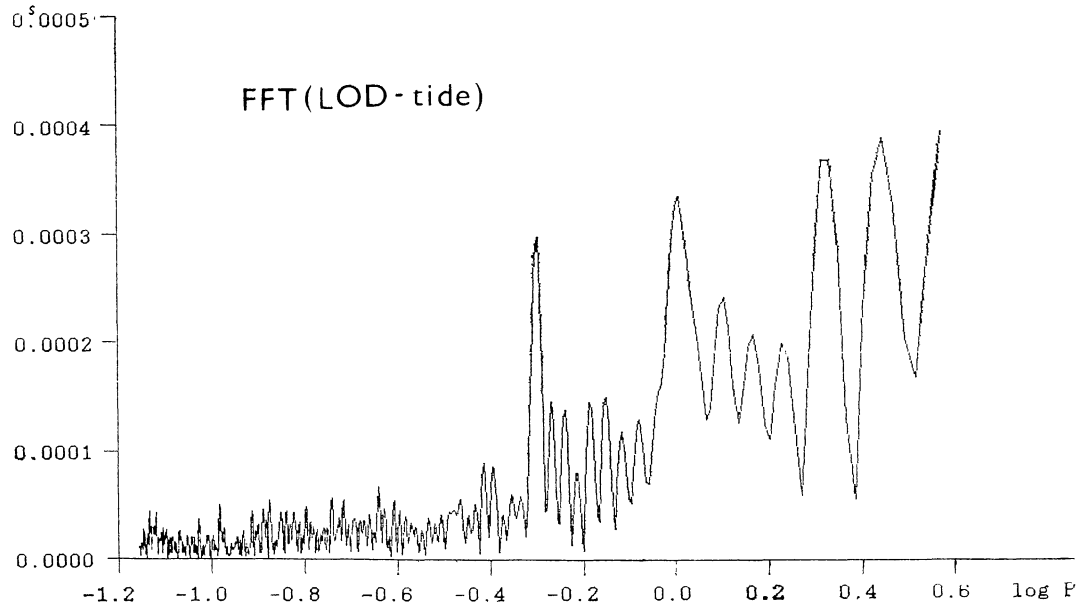

Fig. 6. The spectrum of the observed LOD with tidal variations removed, calculated by the FFT.

were considered – the spectrum would be distorted for shorter periods:

i) The Fast Fourier transform (FFT), which is known to produce sidelobes, placed symmetrically at both sides of any dominant peak of the spectrum. The sidelobes necessarily have a slight effect on the neighbouring peaks.

ii) The much slower method of least squares (MLS), by which we derived the amplitude and phase of the sinusoidal wave whose period was changed stepwise over a given range of periods. Since a simple relation between LOD and χ_3 should theoretically exist (Barnes et al 1983),

$$\text{LOD} = \chi_3 + \text{constant}, \tag{4}$$

both spectra are directly comparable.

2.1 *FFT Spectra Analysis*

The amplitude spectra obtained with the FFT technique are plotted in Figs 5–8, in which the horizontal scale is logarithmic (period in years) and the vertical in seconds of time. Figure 5 shows the

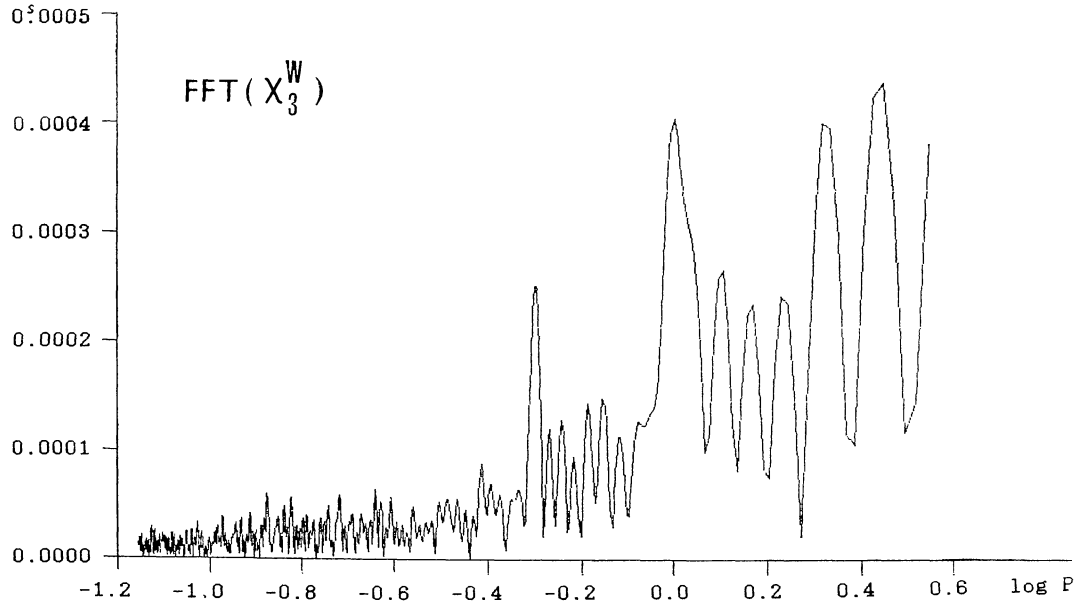

Fig. 7. The spectrum of the axial component of the wind term of the atmospheric EAMF, calculated by the FFT.

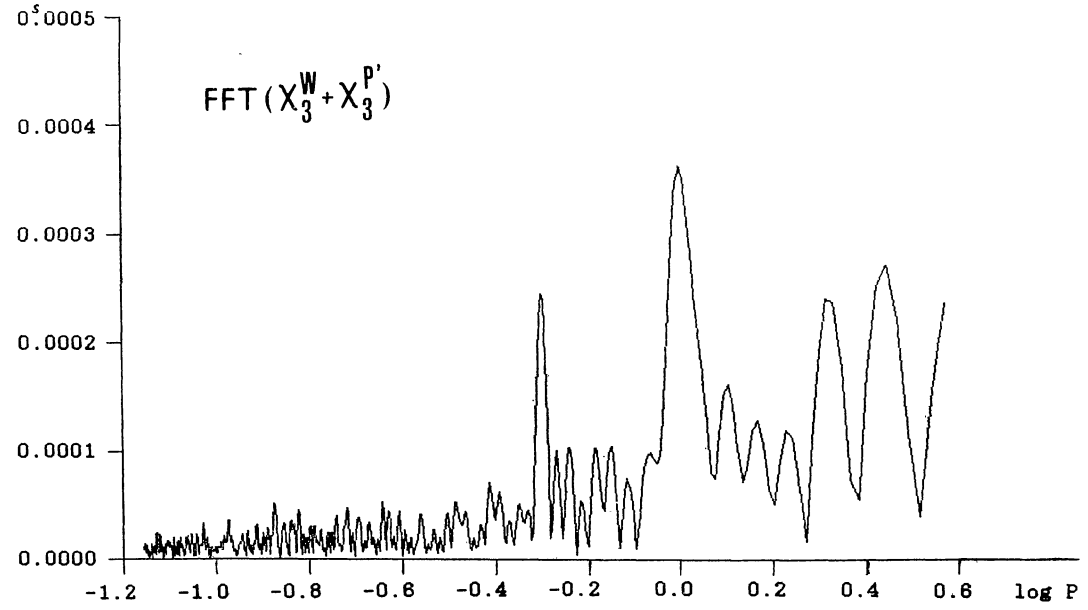

Fig. 8. The spectrum of the axial component of the sum of the pressure and wind terms of the atmospheric EAMF, calculated by the FFT.

spectrum of the observed LOD changes. Far to the left there is a large peak of the monthly term, evidently of tidal origin. Dominant are semi-annual and annual terms, and also two terms of longer periods, equal to 2 years and 2·7 years. A similar pattern can be seen in Fig. 6, where the theoretical tides with $k/C = 0{\cdot}94$, after Yoder et al. (1981), have been removed. The monthly term has disappeared and the amplitudes of the two dominating terms are slightly reduced. The remaining fine structure of the spectrum is nearly identical with Fig. 5, because there is practically no significant tidal term with a period between one month and half a year, and also between 1 y and 18·6 y. The spectrum of the wind term is displayed in Fig. 7. It is very similar to the spectrum of LOD without the tidal terms (compare Figs 6 and 7), especially for periods shorter than half a year. Nevertheless, there are differences in the two most pronounced terms – the amplitude of the semi-annual term is slightly smaller, and the amplitude of the annual term is larger than the observed value. The pattern improves if the pressure term is added; the amplitude of the semi-annual term remains practically the same, but the amplitude of the annual term is smaller, thus coming closer to the observed value (Fig. 8). Substantially diminished are the long-periodic terms.

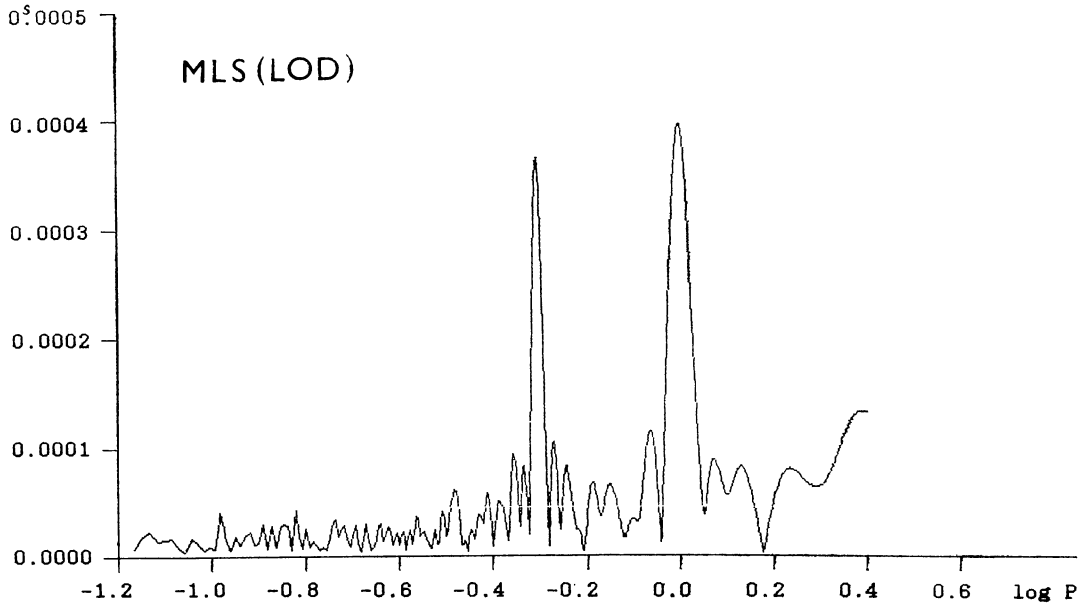

Fig. 9a. The spectrum of the observed LOD, calculated by the method of least squares, with resolution in period of 1d.

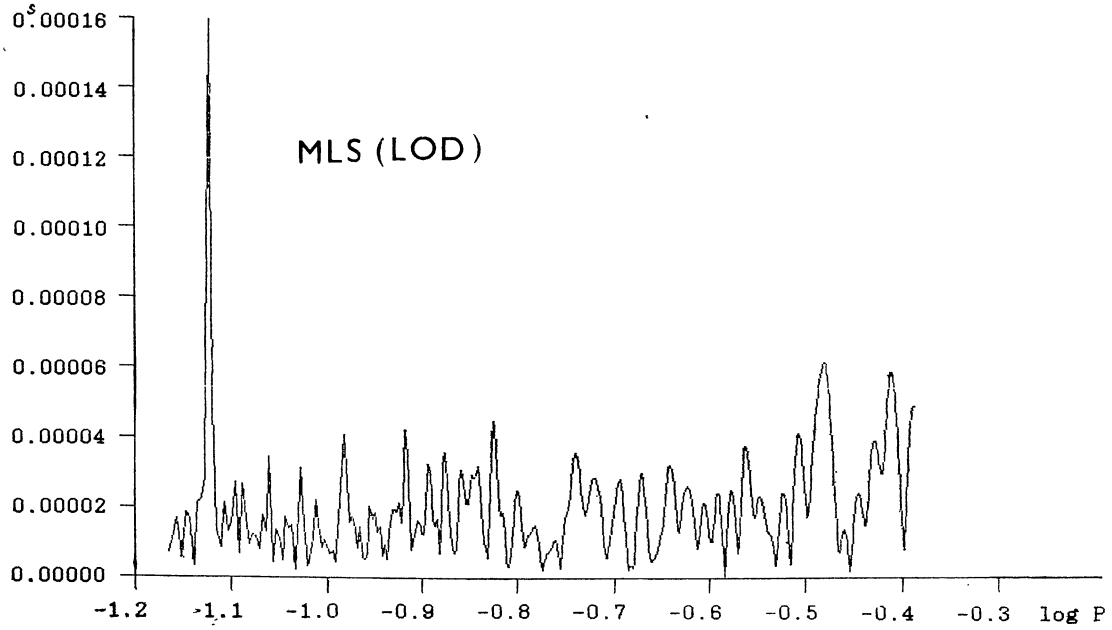

Fig. 9b. Short-periodic part of the LOD spectrum, calculated by the method of least squares, with resolution in period of 0·25 d.

2.2 *MLS Spectral Analysis*

The results of the spectral analysis, carried out with the least-squares method, are graphically displayed in Figs 9–11. Figures 9a and 9b show the spectrum of the observed LOD; Fig. 9a the spectrum in the whole period range, i.e. from 25 days to 2·5 years, with a period resolution of 1 day, and Fig. 9b the spectrum with a finer resolution (0·25 days) for the shorter period range (from 25 days to 150 days), on an enlarged vertical scale. The spectrum is quite similar to the FFT (LOD) spectrum in Fig. 5, but for the annual peak (which is a little higher here) and for the long-periodic part (that is almost completely missing). Nearly the same situation as in the case of FFT can be seen in Figs 10a and 10b, in which the tides have been removed – the amplitudes of both the semi-annual and annual terms are a little bit smaller and the monthly term has almost completely disappeared. The analysis of the wind term of the EAMF alone is not shown here simply because there is no substantial difference between it and the combination of wind and pressure terms, depicted in Figs 11a and 11b. If these two spectra are compared with those of Figs 10a and 10b, we can see that they are very similar. There are again some differences

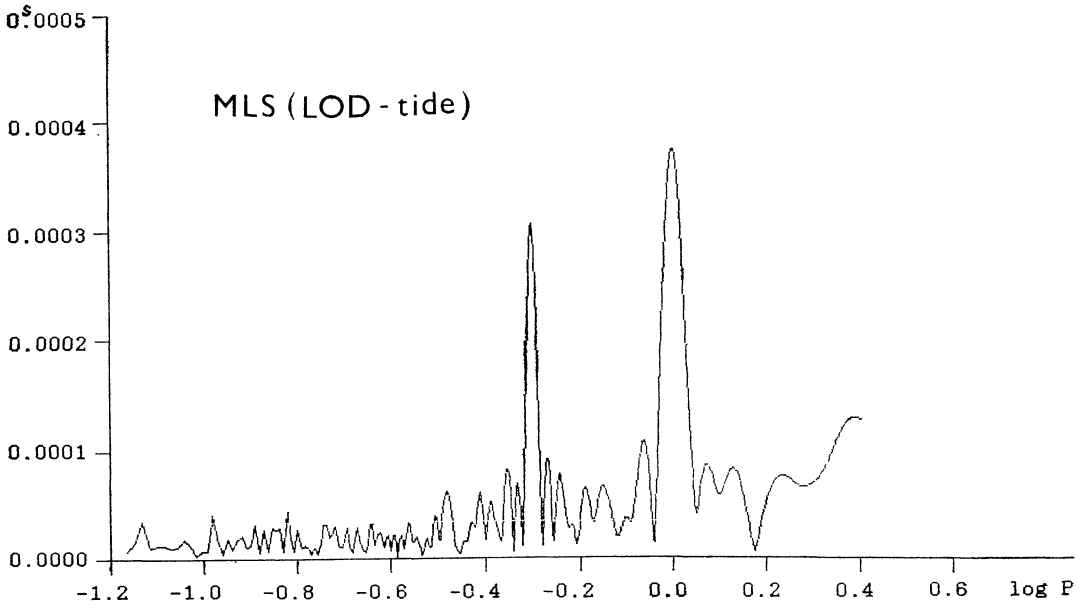

Fig. 10a. The same as Fig. 9a, with tidal variations removed.

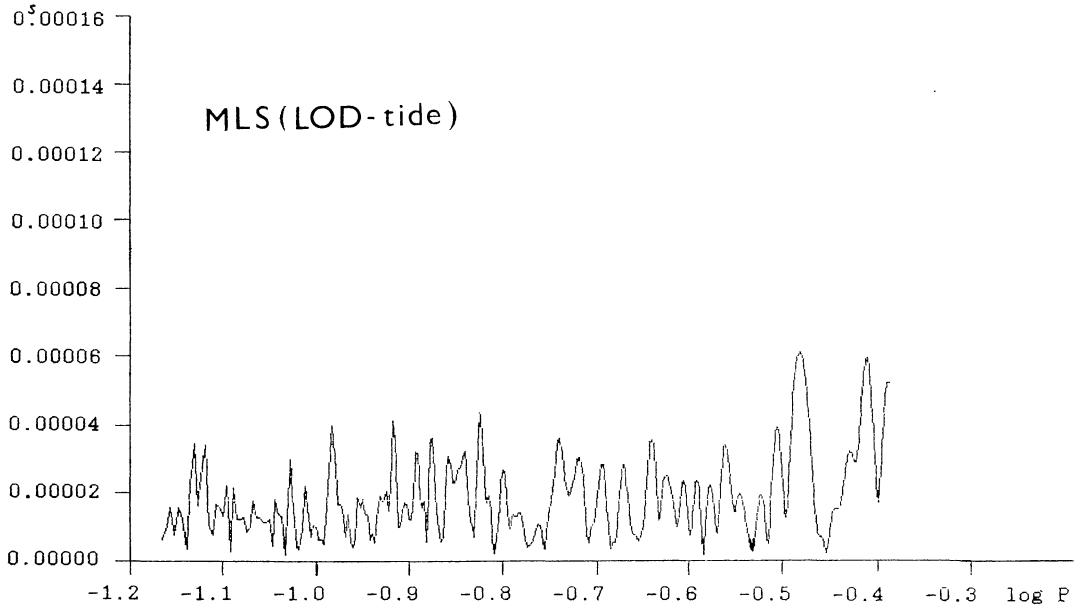

Fig. 10b. The same as Fig. 9b, with tidal variations removed.

in the amplitudes of semi-annual and annual terms (the observed amplitude of semi-annual term is larger than the amplitude expected due to atmospheric excitation, while the observed amplitude of the annual term is smaller), but the spectra are surprisingly identical for periods shorter than 150 days (compare Figs 10b and 11b).

In comparing the FFT and MLS spectra, one can see that the FFT method highly exagerates the amplitudes of the long-periodic terms with respect to MLS. These terms, if they really exist, are probably much smaller and their atmospheric origin is doubtful. On the other hand, both methods reliably disclose a high number of periodic terms not only in the well-known range between 50 and 70 days, but also for longer periods. An overview of all the periods detected is given in Tab. 1. The periods in days, given in the first column of the table, are average values obtained of all the four analyses, as displayed in Figs 6, 8, 10 and 11. Except for the most significant annual and semi-annual terms, 22 terms have been detected. All of them are present both in the FFT and MLS

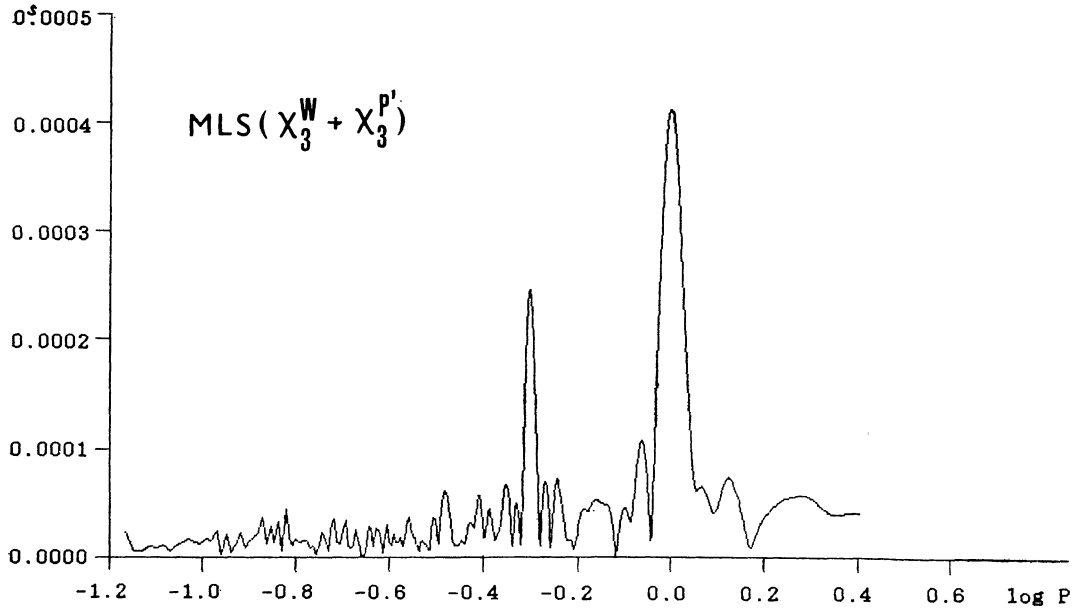

Fig. 11a. The spectrum of the axial component of the atmospheric EAMF, calculated by the method of least squares, with resolution in period of 1d.

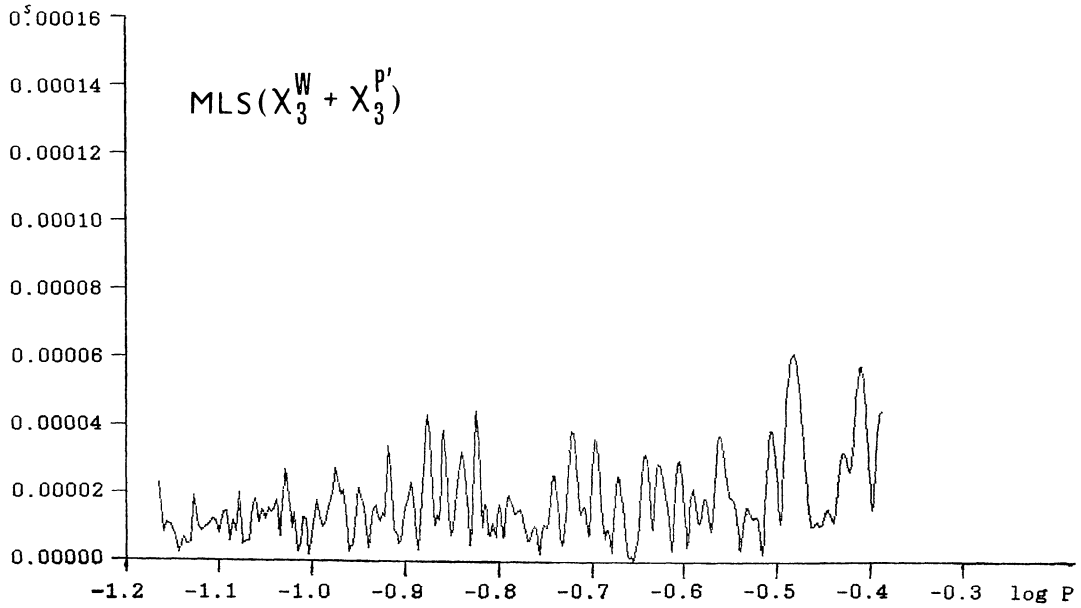

Fig. 11b. The spectrum of the axial component of the atmospheric EAMF, calculated by the method of least squares, with resolution in period of 0·25 d.

Table 1

Periodic terms up to 1 year found by spectral analysis in LOD and axial atmospheric EAMF

Period in days	Amplitude FFT LOD	FFT EAMF	MLS LOD	MLS EAMF
34·1	0·000038	0·000038	0·000030	0·000027
38·4	50	50	40	27
44·4	43	44	41	34
47·0	45	28	32	23
48·7	54	54	36	43
51·0	43	33	31	39
52·8	44	35	32	32
54·8	43	43	43	44
58·2	48	49	27	17
66·6	57	57	35	26
70·0	54	55	31	39
73·9	36	38	29	37
78·0	36	33	28	26
83·8	67	67	35	32
86·3	47	43	25	29
90·6	54	54	24	30
100·2	34	41	34	37
114·2	41	43	34	38
120·2	45	46	61	61
125·8	55	57	—	—
141·8	90	89	60	58
149·3	87	87	52	44
182·6	293	246	306	246
365·2	328	363	375	412

analyses, save for the term with the period equal to 125·8 days, which is present only in FFT analysis. This term is very probably an artefact due to the leakage of sidelobes from the dominant terms. A surprisingly excellent agreement between the observed amplitudes (headed as LOD) and amplitudes expected due to atmospheric excitation (headed as EAMF) for periods between 30 and 150 days witness that, for this part of the spectrum, all the observed variations in the rotational rate of the Earth can be ascribed to atmospheric excitation. None of this is changed by the obvious fact that the MLS analysis tends to yield systematically smaller amplitudes (both for LOD and EAMF) than FFT. The situation is not that clear with the dominating semi-annual and annual terms. It is very probable that the discrepancies here are mainly due to the higher layers of the atmosphere neglected in the NMC data. The wind term is not in fact calculated for the whole volume of the atmosphere, as it should be, but rather only up to the pressure level of 50 mbars, as discussed by Rosen and Salstein (1985). In analysing the contribution of stratospheric winds on the interval 1980–1981 they found that the annual component in the stratosphere is approximately 180° out of phase with that in the troposphere, while for the semi-annual component they are roughly in phase. Thus the stratosphere acts to decrease the amplitude of the annual component by about 0·060 msec and to increase the amplitude of the semiannual component by about 0·047 msec. These numbers can almost fully explain the difference between atmospheric excitation and the observed LOD changes in Tab. 1. Other possible sources of excitation at these two frequencies could be groundwater storage changes (but these are very small), sea-level changes or ocean currents (which are not sufficiently well known) – for a detailed discussion refer to (Lambeck, 1980).

3. Atmosphere and Tides versus LOD

Now it is clear that the variations in LOD are, at least at high frequencies (i.e. higher than 1 cpy), mostly driven by the combination of tidal deformations of the Earth's body and the redistribution of angular momentum between the solid Earth and its armosphere. The scaling factors for both effects are certain functions of some of the parameters, characterizing the real Earth. To begin with the tides, the scaling factor which is used to multiply theoretical amplitudes after Yoder et al. (1981) is equal to k/C, where k is the elastic Love number of the Earth and C is the dimensionless polar moment of its mantle's inertia. As for the axial component of the atmospheric EAMF, the scaling factor is multiplied by $1 + k'$ for the pressure term and 1 for the wind term, where k' is the load Love number; they both also depend on certain constants preceding the integrals in Eqs (2) and (3). So far we have used the values $k/C = 0{\cdot}94$, $1 + k' = 0{\cdot}70$. In the following, we shall determine new values of the scaling factors, using the time series of LOD and EAMF studied above. Namely, we shall try to fit the LOD, expressed in terms of tidal and atmospheric excitation as

$$(5)\quad \mathrm{LOD}_c = a + bt + ct^2 + d(\chi_3 - \chi_0) + e(tide)$$

to the observed values LOD_0. The unknown coefficients $a - e$ can be derived by the method of least squares to satisfy the condition

$$(6)\qquad (\mathrm{LOD}_c - \mathrm{LOD}_o)^2 = \text{minimum}\,.$$

Coefficients $a - c$ are meant to express the approximation of the decade fluctuations of LOD in the interval studied, while d and e are the scaling factors we are looking for. t denotes the time in Julian years elapsed

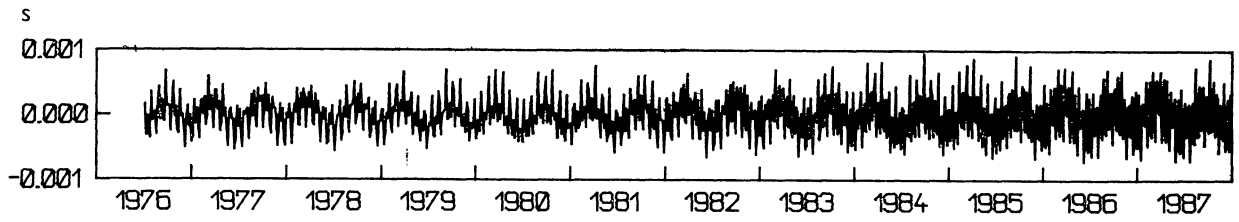

Fig. 12. Tidal variations in LOD with scaling factor $k/C = 0{\cdot}945$. Only the terms with periods less than 8 y have been considered.

since MJD = 4 5061·5, i.e. $t = (\text{MJD} - 45\,061{\cdot}5)\,/\,/\,365{\cdot}25$ and χ_0 is the mean value which is removed from the atmospheric EAMF before solving, i.e. $\chi_0 = 14{\cdot}149 \times 10^{-7}$. In order to convert the EAMF values to LOD changes in seconds of time, they must be multiplied by 86 400. Since the interval studied is too short to enable the analysis of very long-periodic tidal variations, only the first 59 terms of Yoder's list have been used to calculate the *tide* in eq. (5); the last three terms with periods longer than 8 years have been omitted. The tidal variations in LOD derived from the 59 terms are depicted, for the interval in question, in Fig. 12. It can be seen that especially the short-periodic terms towards the end of the interval have very large amplitudes – these are caused by the interference of the two large fortnightly terms with arguments $2F + \Omega$ and $2F + 2\Omega$ (and with close periods of 13·63 and 13·66 days, respectively) which were in phase in November 1987. The observed values of LOD used for this analysis are based on the latest BIH combined solution ERP(BIH) 87 C 02 (Feissel and Guinot 1988), in the interval 1976·5–1988·0. In order to investigate the possible influence of the adjusted tidal scaling factor e on the value k/C actually used to calculate LOD_0 from the observed UT1 – TAI values (see Section 2), the whole solution was repeated several times, with different values of k/C used to derive LOD_0. The results are graphically displayed in Fig. 13, in which the solid line shows the dependence of e on k/C and the dashed line is given by the equation $e = k/C$. The intersection of both lines determines the most probable value of the adjusted coefficient e, i.e. $e = 0{\cdot}945$. Namely this value was then used for k/C in calculating LOD from the observed values UT 1 – TAI in the final solution. The adjusted values of the unknowns $a - e$ are shown, together

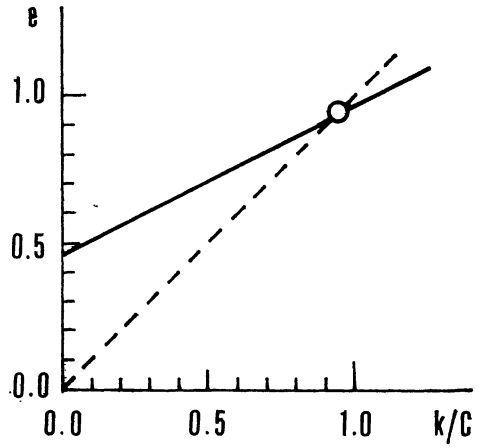

Fig. 13. The dependence of the adjusted tidal scaling factor e on its value used to calculate LOD from the UT 1–TAI values.

with their mean errors, in Tab. 2. The coefficients of correlation between the individual adjusted values, also displayed in the table, are evidence that there is no dangerous correlation in the system of normal equations. This especially holds for the unknowns d and e determined practically independently of one another (the corresponding coefficient of correlation

Table 2

Adjusted values of the unknowns approximating the best fit of LOD changes by the combination of atmospheric exciation and zonal tides after eq. (5)

Unknown	Adj. value	Mean error	Coefficients of correlation				
			a	*b*	*c*	*d*	*e*
a	0·002152	±0·000011	1·00				
b	−0·0001589	±0·0000022	0·00	1·00			
c	−0·00000472	±0·00000072	−0·75	0·00	1·00		
d	0·943	±0·018	0·04	0·06	−0·05	1·00	
e	0·945	±0·021	0·00	0·00	0·00	−0·06	1·00

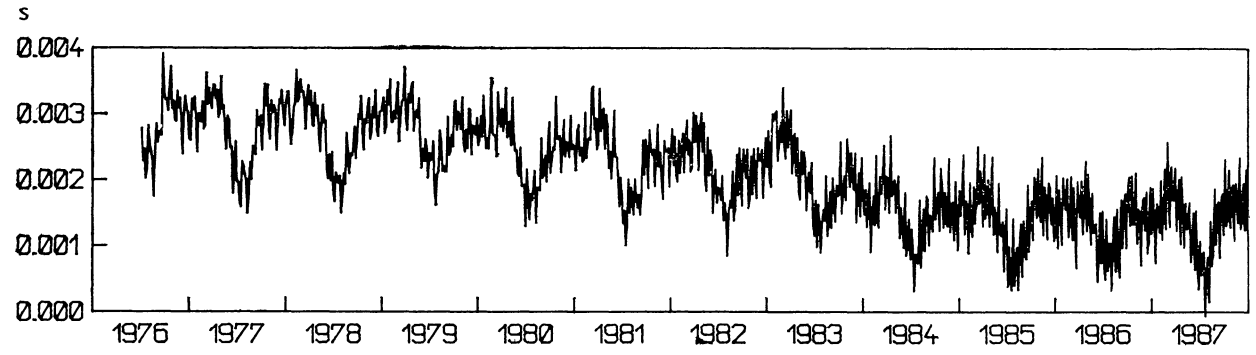

Fig. 14. LOD changes, calculated from the atmospheric excitation and tidal effects using eq. (5).

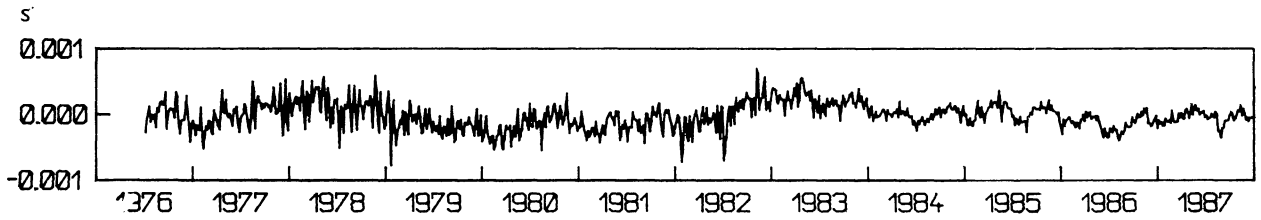

Fig. 15. The differences between the observed (Fig. 1) and calculated (Fig. 14) LOD.

being equal to only −0·06). Fig. 14 shows the resulting LOD_c changes, calculated using formula (5) and the numerical values from Tab. 2. It is obvious that the curve is nearly identical with the curve displaying the observed values LOD_0 (compare with Fig. 1); the difference between LOD_0 and LOD_c is plotted in Fig. 15. It clearly demonstrates the gradual improvement of the fit, especially after 1983, when the new space techniques started to dominate in the observed Earth rotation parameters. The UT 1 component, based until 1978 uniquely on optical astrometry, was also observed by lunar laser ranging after this date, and after 1982 it was VLBI that gradually attained higher and higher relative weight. The average root-mean-square difference between the two LOD representations, calculated over the whole interval studied, is equal to ±0·00021 sec.

The spectral analysis of the residuals from Fig. 15, carried out by the FFT method, is shown in Fig. 16. Clearly visible are the semi-annual and annual peaks most probably caused by the neglected stratospheric winds (see also the discussion at the end of Section 2). The other two dominant peaks at periods of 2·4 y and 6·0 y are evidently of an origin different than the atmos-

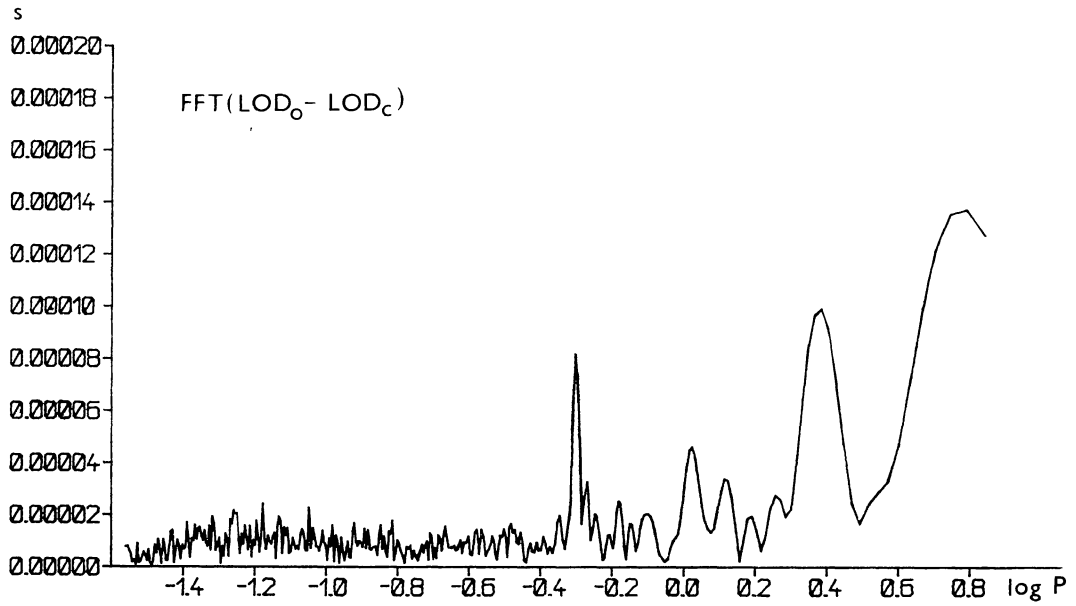

Fig. 16. FFT spectrum of the differences between the observed and calculated LOD.

pheric or zonal luni-solar tides. The spectrum for periods shorter than 0·5 y clearly demonstrates the obvious fact that the rotation of the Earth at these frequencies can be fully explained by the combined effect of the atmosphere and Earth tides; no additional perturbation wave in the range between 13·5 d and 13·8 d, found by Capitaine and Guinot (1983), can be seen in the spectrum.

4. Concluding Remarks

The present study shows that there is practically no additional excitation to the atmosphere and tides for periods of less than 180 days; the spectrum in Fig. 15 depicts only noise in this frequency range. The small discrepancies in amplitudes of the semi-annual and annual components can very probably be ascribed to stratospheric winds, neglected in the NMC analysis, but this would call for a more detailed investigation, based on data covering an interval longer than the two-year interval used by Rosen and Salstein (1985). On the other hand, there exist variations of longer period in LOD (with periods 2·4 y and 6·0 y and amplitudes 0·10 msec and 0·14 msec respectively) which can be explained neither by the atmosphere, nor by the Earth tides. Here, not unlike in the case of the well-known decade fluctuations, another source of excitation must be present. The scaling factor found for the influence of the atmosphere ($0{\cdot}943 \pm 0{\cdot}018$) seems to show that the constants preceding the integrals in Eqs (2) and (3) should be a little smaller than used by the NMC (compare this number with the scaling factor of 0·993 obtained theoretically by Vondrák 1987). On the other hand, it is certain that the adjusted value of the atmospheric scaling factor depends on the amplitudes of the dominating atmospheric seasonal terms – if the stratospheric winds were included, the adjusted scaling factor would surely change. The obtained tidal scaling factor k/C ($0{\cdot}945 \pm 0{\cdot}021$) fully confirms, and even defines more precisely, the value recommended by Yoder et al. (1981). Better agreement between the observed LOD variations and those calculated from the tides and atmospheric EAMF achieved after 1983 (see Fig. 15) proves that errors of astronomical observations are mainly responsible for the noise of the differences at higher frequencies. The new observing techniques now used will, therefore, lead to a better understanding of the character of the missing excitation in the near future.

REFERENCES

Barnes R. T. H., Hide R., White A. A., Wilson C. A., 1983 *Proc. Roy. Soc. London A* **387**, 31

BIH 1977—1986 *Annual Reports for 1976—1985*, Bureau International de l'Heure Paris

Capitaine N., Guinot B. 1983 Anomalies of Some Tidal Waves of UT 1, Presented at the IAG *Symp. Geodynamics Aspects of Earth Rotation* Hamburg

Dickey J. O., Eubanks T. M. 1987 in Holota P. (Ed.): *Proc. Internat. Symp. Figure and Dynamics of the Earth, Moon and Planets* (Astr. Inst. and Res. Inst. Geod., Praha), 907

Djurovič D., Pâquet P. 1988, *Astron. Astrophys.* **204**, 306

Eubanks T. M., Steppe J. A., Dickey J. O., Callahan P. S. 1985 *J. Geophys. Res.* **90**, B 7, 5385

Fallon F. W. 1986 Magnetic tape with EAMF, priv. comm.

Feissel M., Guinot B. 1988 *BIH Annual Report for 1987*, Bureau Internat. de l'Heure Paris et Sèvres, D-79

Feissel M., Nitschelm Ch. 1985 *Ann. Geophys.* **3**, 181

Gambis D. 1988 Magnetic tape with ERP and EAMF, priv. comm.

Lambeck K., Cazenave A. 1973 *Geophys. J. Roy. Astron. Soc.* **32**, 79

— 1974 *Geophys. J. Roy. Astron. Soc.* **38**, 49

— 1977 *Phil. Trans. Roy. Soc. London A* **284**, 495

Lambeck K. 1980 *The Earth's Variable Rotation: Geophysical Causes and Consequencies* (Cambridge Univ. Press)

Munk W. H., MacDonald G. J. F. 1960 *The Rotation of the Earth: A Geophysical Discussion* (Cambridge Univ. Press)

Rosen R. D., Salstein D. A. 1983 *J. Geophys. Res.* **88**, C 9, 5451

— 1985 *J. Geophys. Res.* **90**, D 5, 8033

Salstein D. A. 1987 *IAG SSG 5—98 Bulletin No. 4*, Section IV

Sidorenkov N. S. 1973 *Izv. AN SSSR, Fizika atmosfery i okeana* **9**, 339

— 1979 *Astron. Zh.* **56**, 187

Vondrák J. 1987 in Holota P. (Ed.) *Proc. Internat. Symp. Figure and Dynamics of the Earth, Moon and Planets* (Astr. Inst. and Res. Inst. Geod. Praha) 1039

Yoder C. W., Williams J. G., Parke M. E. 1981 *J. Geophys. Res.* **86**, B 2, 881